

The physics behind groundwater recession and hydrologically passive mixing volumes.

Baibaswata Bhaduri¹, Ophelie Fovet³, Sekhar Muddu^{1,2} and Laurent Ruiz^{2,3}

¹Indian Institute of Science, Bangalore, India.

²Indo-French Cell for Water Sciences, Indian Institute of Science, Bangalore, India.

³INRAE, Institut Agro, UMR SAS, Rennes, France.

Corresponding author: Baibaswata Bhaduri (baibaswatab@iisc.ac.in / baibaswatabhaduri@gmail.com)

Key Points:

- Synthetic Dupuit-Forchheimer box aquifers resembling the behaviour of lumped model units (linear reservoir + dead storage) were generated.
- Equivalence relations were established between conceptual and conventional groundwater parameters via parameter influence analysis.
- Procedure to run forward flow and transport simulations in ungauged catchments using lumped models was outlined.

Abstract:

To estimate groundwater flow and transport, lumped conceptual models are widely used due to their simplicity and parsimony – but these models are calibration reliant as their parameters are unquantifiable through measurements. To eliminate this inconvenience, we tried to express these conceptual parameters in terms of hydrodynamic aquifer properties to give lumped models a forward modelling potential. The most generic form of a lumped model representing groundwater is a unit consisting of a linear reservoir connected to a dead storage aiding extra dilution, or a combination of several such units mixing in calibrated fractions. We used one such standard two-store model as our test model, which was previously nicely calibrated on the groundwater flow and transport behaviour of a French agricultural catchment. Then using a standard finite element code, we generated synthetic Dupuit-Forchheimer box aquifers and calibrated their hydrodynamic parameters to exactly match the test model's behaviour (concentration, age etc). The optimized aquifer parameters were then compared with conceptual parameters to find clear physical equivalence and mathematical correlation – we observed that the recession behaviour depends on the conductivity, fillable porosity, and length of the catchment whereas the mixing behaviour depends on the total porosity and mean aquifer thickness. We also noticed that for a two-store lumped model, faster and slower store represents differences only in porosities making it rather a dual porosity system. We ended with outlining a clear technique on using lumped models to run forward simulations in ungauged catchments where valid measurements of hydrodynamic parameters are available.

1. Introduction:

Transit time distributions give us insights on the behaviour of water and solutes within a hydrological system (Hrachowitz et al., 2016). Transit time estimation has thus become a common tool of process representation in flow and transport models in recent times, and a strong test of model output realism (Benettin et al., 2022). But certain aspects of transit time theory still come under the “unsolved problems” in hydrology (Blochl et al., 2019). Subsurface water is an important medium for transporting geochemical constituents on a global scale. But unlike surface water, subsurface water is not easy to access and quantify, and water and solute fluxes through subsurface systems are very difficult to measure (Phillips and Castro, 2003). However, intensification of agriculture and the resultant increment in application of nitrate rich products in agricultural catchments for the past few decades has dramatically increased the legacy nitrate concentration in both vadose zone and groundwater along with nitrate loading in streams (Galloway et al., 2004; Seitzinger et al., 2010; Howden et al., 2011; Worrall et al., 2012; Dunn et al., 2012; Ehrhardt et al., 2019) leading to global

issues like the nitrate time-bomb problem (Wang et al., 2013), and exceedance of the planetary boundary by the nitrogen cycle (Rockstorm et al., 2009). The attenuated response of legacy nitrogen stored in deeper groundwater compartments often causes catchments to take several decades to flush out existing nitrates (Martinec, 1975; Ruiz et al., 2002; Tomer and Burkart, 2003; Basu et al., 2010; Meals et al., 2010; Stewart et al., 2010; Aquilina et al., 2012; Basu et al., 2022) resulting in a very long timescales to reflect managerial measures on stream nitrate concentration. It is thus necessary to estimate the solute release rate of catchments by modelling groundwater and solute transit time, and it has been thus prevalent in hydrology for a very long time (Maloszewski and Zuber, 1982; Goode, 1996; Etcheverry and Perrochet, 1999; Kirchner et al., 2000; Duffy, 2010; Gilmore et al., 2016; Bhaduri et al., 2022a). Therefore, a lot of advances have been made in catchment scale flow and transport modelling in the last couple decades (McGuire and McDonnell, 2006; Hrachowitz et al., 2016; Benettin et al., 2022). Amongst these, physics-driven distributed hydrological models like MODFLOW-MT3D (McDonald and Harbaugh, 2003; Zheng et al., 2012), PARFLOW (Kollet and Maxwell, 2006), FEFLOW (Diersch, 2013) etc can most accurately simulate catchment flow and transport processes whilst being able to account for the process complexity and heterogeneity. But such models have a large computational expense, and they still deal with ill-posedness in inverse problem definition (Hrachowitz et al., 2016; Bhaduri et al., 2022b). Consequently, reliance in parsimonious lumped conceptual models was reaffirmed in recent times (Birkel et al., 2014; Fovet et al., 2015) primarily due to adaptability and computational simplicity, despite having issues like lack of physical basis, non-scalability and inability to forward model (Hrachowitz et al., 2016; Bhaduri et al., 2022b). But the question of whether these models will be able to imitate realistic catchment processes and in turn accurately determine the transit times and produce “right answers for the right reasons” still remains (Kirchner, 2006; Hrachowitz et al., 2013). Furthermore, long-term time series measurements of groundwater levels and solute concentrations is a very daunting task and there are many catchments in the world which lack such extensive measurement (Li et al., 2021) – but it is essential to calibrate lumped models. Therefore, there are new avenues to explore about the linkage of the lumped conceptual parameters to measured realistic field parameters giving hydrologists some perspectives of forward modelling using lumped models and using them as a prediction tool and not just a calibration tool.

There are multiple ways to improve the transit time predictive performance of lumped conceptual models. In terms of data, enabling the model to use long-term discharge and concentration time series of the streams, as well as long term groundwater storage and chemical or tracer information will help to constrain the model better and yield better results (Seibert and McDonnell, 2002; Gupta

et al., 2008; Fovet et al., 2015; Bhaduri et al., 2022a). In terms of process representation, using different static and dynamic mixing coefficients that represent different fractions of input water mixing with resident water (Dunn et al., 2007, Fenicia et al., 2010; McMillan et al., 2012; Soulsby et al., 2015; Birkel et al., 2015) has been quite beneficial, which eventually led to the development of piecewise linear SAS functions (Benettin et al., 2022). One step forward could be an attempt to generate physically equivalent systems resembling conceptual lumped stores, and analyze those systems to understand the physics of the conceptual stores and explore the insights that these stores are providing about the emergent properties of the catchment. This might reduce the calibration dependency of lumped models and provide opportunities to inspect effectiveness of conceptual parameters.

Lumped conceptual models usually represent groundwater as a linear reservoir (or a weighted combination of multiple linear reservoirs). Each reservoir has an unique recession coefficient, which is a measure of the rate or speed at which the reservoir releases water, the rate being the inverse of its turnover time. These reservoirs are usually attached to an immobile volume / dead storage which aids the additional dilution required for the input mass to reach the measured levels of concentration of the output breakthrough. These parameters are conceptual and can only be calibrated through inverse modelling. Savenije (2018) mathematically connected Darcy law of groundwater flow to linear reservoir theory. He further mentioned that predicting solute transport in such systems is “much less straightforward requiring assumption of dual porosities”. This inspired us in attempting to establish a mathematical relationship between empirical calibration parameters of lumped models to physical and measurable hydrodynamic aquifer properties that are used as parameters in conventional groundwater flow and transport equations. To do this, we decided to take a synthetic approach. Our objective here is to calibrate the parameters of a standard finite element code solving Boussinesq and advection-dispersion equations against the outputs of a standard linear reservoir model, which was previously calibrated against the data of a real world catchment with high degree of accuracy. The parameters that we obtained from the exact calibration of a complex and process-intensive model against the outputs of a parsimonious model will give us an exhaustive understanding of three things: (a) parametric equivalence, i.e., to find a proper physics-based explanation on how this generic unit cell (linear reservoir + dead storage) parameters are efficiently reproducing correct groundwater flow and transport behavior; (b) parametric disparity, i.e., to check if two parameters are apparently somewhat equivalent in process reproduction but due to different physical reasons. (c) whether the age distribution of groundwater of the distributed model agrees with the nitrate travel times of the

lumped model since both are representative of particle movement timescales. If clear and generic mathematical connections are established, it can create a forward modelling potential for both flow and transport in lumped models, which would be beneficial for catchments with no long-term time series available for calibration. It will also improve calibration performance due to prior knowledge on the parameter ranges.

2. Materials and Methods:

2.1 Study site, observation and modelling data used:

Kerrien (Figure 1) is a 10.5 ha agriculture dominated headwater catchment located in the Kerbernez site of South-Western French Brittany (47°35' N; 117°52' E), which belongs to the AgrHys Critical Zone Observatory (Fovet et al., 2018; https://www6.inra.fr/ore_agrhys_eng/). For the detailed description of topography, climate, soil, data monitoring and surveys conducted on Kerrien please refer to Fovet et al., 2015.

ETNA (Ruiz et al., 2002) is the most basic form of a linear reservoir model representing groundwater. In this model, two linear reservoirs + dead storage units operate exclusively – the one with faster recession and lesser dead storage is called the fast store and the one with slower recession and higher dead storage is called the slow store. Daily forcing variables are recharge and the solute concentration of recharge, taken from Fovet et al., 2015 (check Supplementary). The outputs of these stores aggregate at the outlet in a calibrated fraction to produce the desired stream nitrate breakthrough. ETNA was calibrated against the long-term nitrate concentration time series (Fovet et al., 2015) of the Kerrien stream outlet, to determine the groundwater flow and transport behavior of Kerrien and the nitrate transit times. Despite its simplicity, it was very good in reproducing the stream nitrate concentration pattern of Kerrien. Based on the optimized parameters of ETNA in Kerrien, Bhaduri et al., 2022a hypothesized that these two reservoirs might be representative of the groundwater from two parallel hillslopes.

FEFLOW 7.5 ([FEFLOW 7.5 Documentation](#)) is the most widely used finite element-based code for solving conventional groundwater flow and transport equations. It is therefore interesting to produce synthetic Dupuit-Forchheimer box aquifers using FEFLOW and calibrate the hydrodynamic parameters against the breakthrough produced by individual ETNA stores hypothetically representing those hillslope aquifers. This synthetic approach will allow us to establish a similarity in

the influence of conceptual and physical parameters and therefore their equivalence. The inputs will be the same as the lumped model, just uniformly distributed.

A brief description of ETNA, and its adaptation to Kerrien is provided in Supplementary. We describe below the analysis that we carried out in a stepwise fashion.

2.2. Stepwise description of procedure followed:

2.2.1. Step 1: Deciding the geometrical configuration of FEFLOW box aquifers:

FEFLOW 7.5 was used to generate synthetic homogeneous box aquifers morphologically equivalent to hypothetical ETNA reservoirs. To do this, equivalence must be established between the physical dimensions of the actual catchment and the Dupuit-Forchheimer aquifers.

In Figure 1, we show that the diagonal of the catchment Kerrien (since Kerrien looks like a rhombus) along the probable mean direction of overall groundwater movement according to the topography and piezometry, is about 385m long (distance of outlet E3 from ridge). We thus decided the dimensions of the rectangular 2D box catchments that we produce will be 400m*270m to match the area of the catchment. The width (W) of 270m does not matter as we took the left and right boundaries to be no-flux boundaries (for both fluid and mass), making the domain behave like an 1d Dupuit-Forchheimer aquifer as shown in Figure 1. The length we have taken is 15 m more than the chief diagonal ($L=385\text{m}$) because the observation point representing the outlet of the catchment should be taken slightly inwards to avoid boundary effects.

A triangular discretization (meshing) was done in the X-Y plane, but due to no-flux boundaries on left and right, and zero transverse dispersivity, both flow and transport was forced along the X-direction (along parallel streamlines). The Upper and the Lower boundaries are thus just representative of $x=0$ and $x=400$ m respectively. Dirichlet boundary conditions for hydraulic head at the upper and lower boundaries are calibrated in accordance with past studies. The Dirichlet boundary conditions for mass is 0 mg/l concentration at both upper and lower boundaries, with a minimum mass flow constraint of 0 mg/l at lower boundary. Like any 1D Dupuit-Forchheimer aquifer, the parabolic head distribution along X from upper to lower boundary represents the curvature of the groundwater table (See Figure 4).

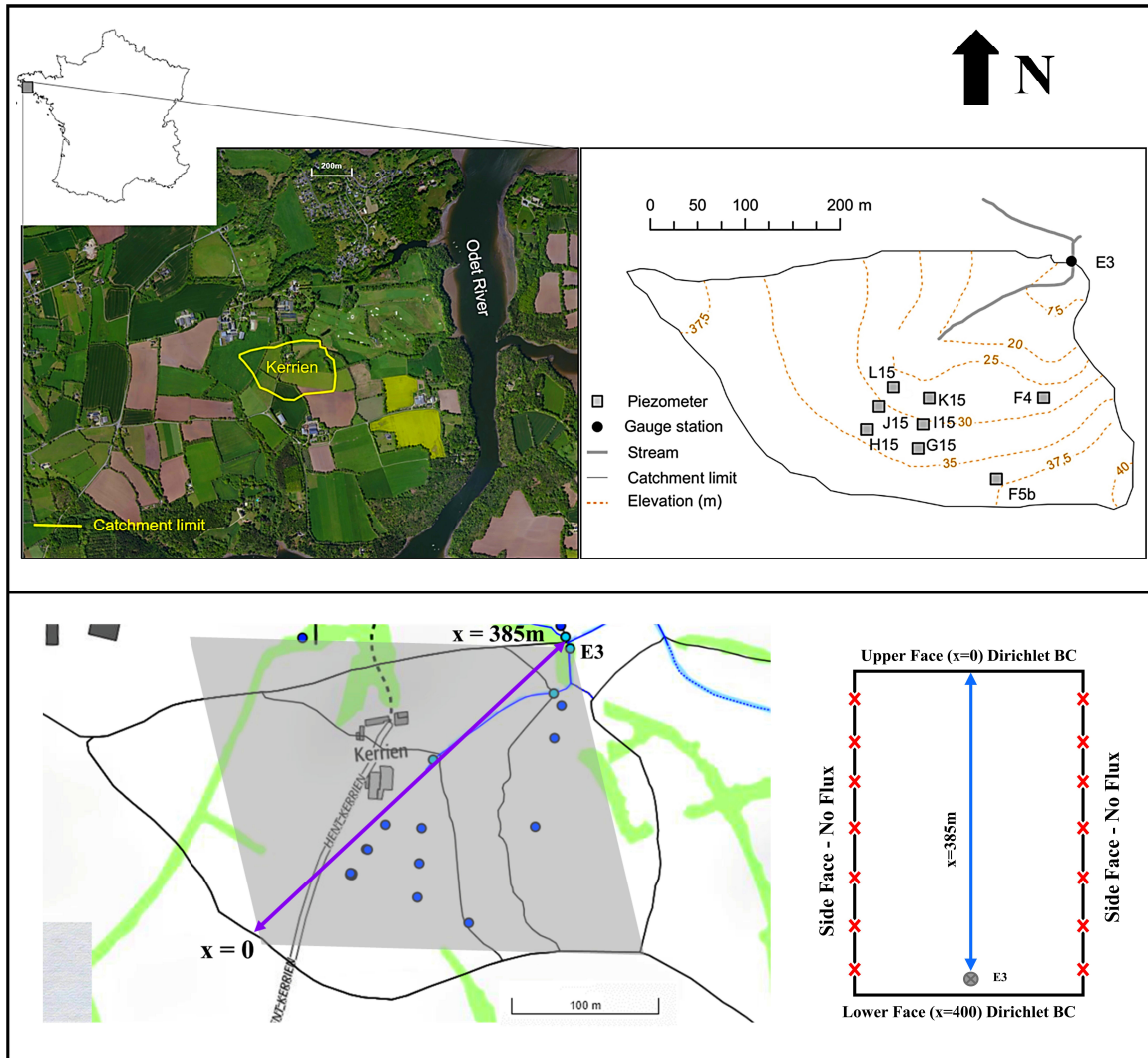


Figure 1: (a) A map of Kerrien catchment (AgrHys Critical Zone Observatory) highlighting important observation locations, stream, catchment limits and elevation contour lines (<https://geosass.fr/agrhys/>) (b) Outline of the diagonal (since Kerrien looks like a rhombus) representing a hypothetical linear stream tube from ridge to outlet E3 along which all the groundwater flow is hypothesized to be taking place. (c) Line-drawing of the basic 2D box aquifer blueprint which is optimized to mimic different ETNA stores.

2.2.2. Step 2: Parameter calibration in FEFLOW 7.5:

We first decide the initial hydrodynamic parameterization of the synthetic box catchments. In the homogeneous representation of Kerrien by Martin et al., 2006, the hydraulic conductivity (K) was taken to be 7×10^{-6} m/s ($=0.605$ m/d). We use this as a starting value. The topographic gradient varied from 14% in the upslope region to 5% in the downslope region, so we took mean hydraulic gradient

(i) of 10% as the value to begin with. The initial value of longitudinal hydrodynamic dispersivity (D) was taken to be 10m (Martin et al., 2006) based on Gelhar's charts (Gelhar et al., 1992). The initial total porosity (η) and drainable porosity (η_f) was taken to be 60% and 5% based on RMS measurements (Martin et al., 2006).

Models like FEFLOW 7.5 produce a hydraulic head field but does not explicitly display discharge, it just displays a nodal and elemental Darcy flux. Furthermore, whether the net discharge will match the discharge of ETNA will largely depend on the method used to calculate the discharge. Thus, the only way to compare the water release rates of the fast and the slow stores of ETNA and corresponding synthetic FEFLOW box aquifers is to compare their discharge recessions. The discharge recession will be different from groundwater head recessions, the estimation technique of which is demonstrated below.

We took 16 equally spaced observation points along the catchment at 25 m intervals, with point 1 and point 16 at 12.5m distance from the boundaries as shown in Figure 3. We simulated the head distribution profiles at those 16 points, and calculated their daily leakages during recessions over the entire simulation period using the following formula:

$$q_L = \frac{\eta_f (h_{t-1} - h_t)}{t (= 1 \text{ d})} \quad \text{Eq(1)}$$

Where q_L is the daily leakage in m/d and h is the head in m. The sum of these leakage time series at all 16 locations, when fit using an exponential decay, will give us a decay constant which is our recession constant.

We optimized our value of K , i and η_f twice (2 realizations, one for fast store one for slow store) in such a way that the mean of such recession constants over the entire simulation period match that of the fast and the slow stores of ETNA. This part of the calibration was done manually by altering K , i and η_f over 2 orders of magnitude – i.e., the range of variations are $0.06 \text{ m/d} \leq K \leq 6 \text{ m/d}$, $0.01 \leq i \leq 1$, $0.005 \leq \eta_f \leq 0.5$, at 5% increments. Here it is important to mention that the choice of the Dirichlet Boundary Conditions at the upper and lower boundaries decides not only the gradient (i), but also the volume available for mixing at a particular location. For instance, a variation of boundary heads from 100m to 50m will produce a different unconfined aquifer thickness than boundary heads varying from 50m to 0m because of difference in volume available for mixing (all

244 other parameters being constant), causing different levels of dilution. We settle for the K , i and η_f
245 that best represents the recession whilst assigning the boundary heads in a way that reproduces the i
246 and at the same time maintains the average thickness of the Dupuit-Forchheimer parabola close to
247 the mean thickness of Kerrien (Martin et al., 2006). We then use the parameter optimization toolbox
248 in FEFLOW (FEPEST) to calibrate the η and fine tune the K and η_f (within the range of manually
249 calibrated parameter values $\pm 5\%$) to capture both the dilution and seasonality of the lumped
250 reservoir output breakthroughs. We then use this K and η_f in reproducing the recessions and check if
251 there's any improvement in results. If yes, we update values of K and η_f , otherwise we keep the
252 values obtained in the last step. We then settle for these K , i , η_f , η with proper Dirichlet BCs at
253 boundaries. A flowchart displaying different steps of this synthetic experiment is outlined in Figure
254 2. Dispersivity (D) was kept at a low value of 10m (as mentioned earlier) as the lumped linear
255 reservoirs of ETNA do not simulate dispersive behavior.

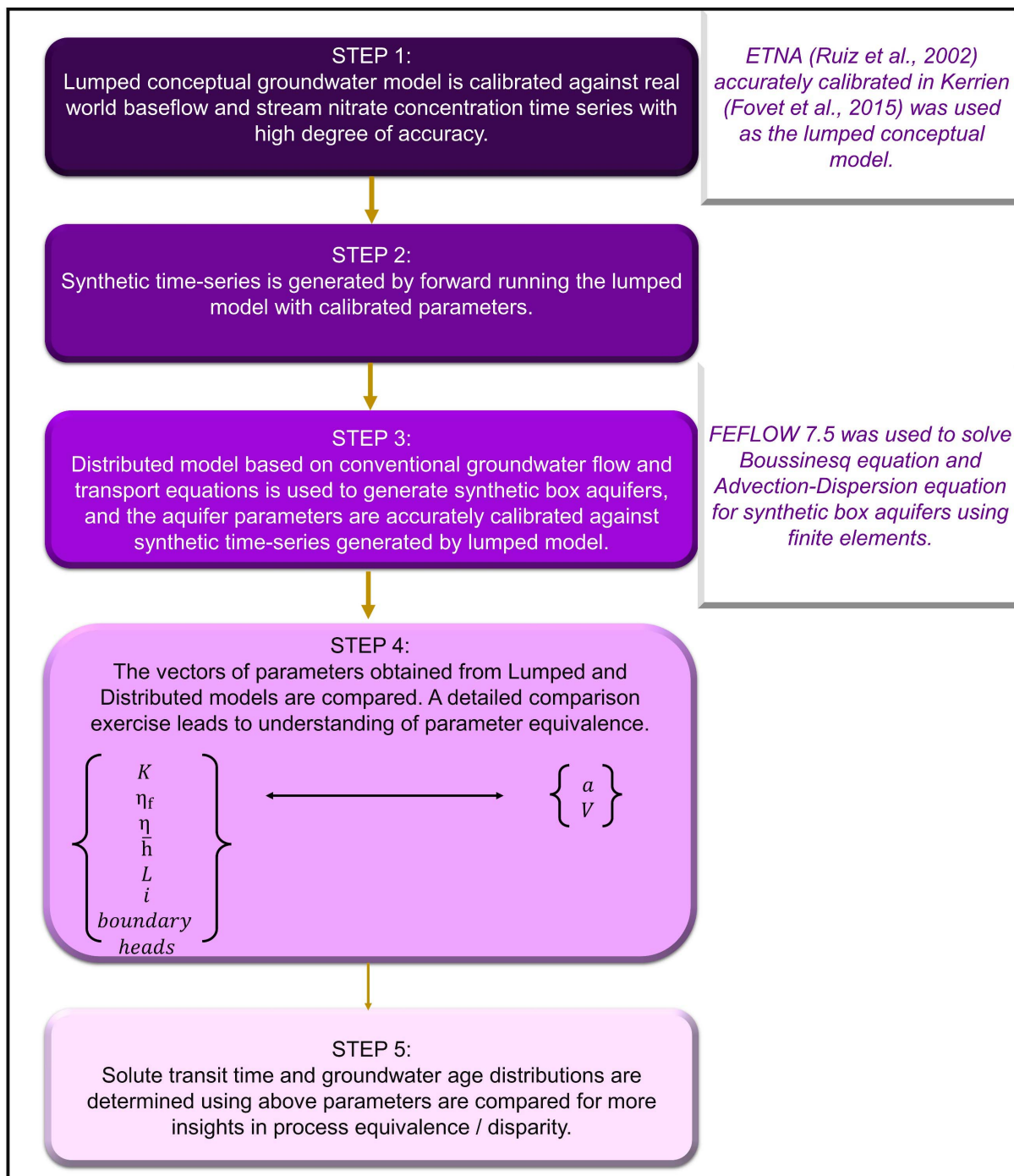


Figure 2: A flowchart illustrating stepwise description of the procedure followed to establish parametric equivalence between conceptual and conventional frameworks.

2.2.3. Step 3: Transit time calculation:

To determine the nitrate transit time using ETNA, same process was followed as Fovet et al., 2015.

Unit pulses of nitrate were sent on 1st August 1968, 1974 and 1980 representative of dry, average and

wet climatic sequences through the calibrated reservoirs. The mean of the times required to recover half the input nitrate at the outlet in all the above 3 cases was calculated as Half Nitrate Recovery Time (HNRT) - which is supposed to be slightly lower than Mean Transit Time (MTT) for long tailed distributions, but nevertheless comparable with groundwater MTT found in the literature.

In FEFLOW we sent an uniformly distributed dirac-delta mass pulse ($1\text{g/m}^2/\text{d}$) on the same 3 dates (1st August 1968, 1974 and 1980) through the finalized box aquifers. We documented the mean movement of the centroid of the output concentration breakthrough, which is the groundwater MTT. For this, the rainfall time series from 2020-2070 was generated just by repeating the time series of 1970-2020.

Furthermore, we calculated the age distribution of the optimized box aquifers. The formula of the mean age is also a centroid calculation formula, and the mean transit time is just the mean age at the outlet. Direct simulation of groundwater age (Goode, 1995) can be done using FEFLOW 7.5 using the following equations:

$$A = \frac{\int_0^{\infty} tCdt}{\int_0^{\infty} Cdt} \quad \text{Eq(2)}$$

$$q\nabla A - \nabla(D\nabla A) = \eta \quad \text{Eq(3)}$$

Equation 3 is derived by substituting Equation 2 in advection-dispersion equation for porous media. $q = (Ki)$ is the Darcy velocity and C is the concentration. The boundary condition for age is very simple – the age is 0 at the inflow boundary (upper boundary). Ideally the HNRT and the MTT will be close to each other. At what point in space of the groundwater age distribution, the age value matches the HNRT and MTT gives us an estimate on the efficiency of lumped models as well as validity of nitrate as an inert (in groundwater) solute in estimating mean travel times of catchment water.

Alteration of the hydraulic conductivity and hydraulic gradient do affect the age distributions to a small degree, but these 2 parameters/variables primarily determine the behavior of mobile water, i.e., they affect the recession, therefore the seasonality. The immobile volumes primarily influencing the long-term behavior or solute transit times are conceptual representations of some physical parameter that aids dilution – it can be dispersivity, 2D hydraulic thickness of unconfined aquifer and immobile

porosity (or a combination). Therefore, we explored the sensitivity of changes in age distribution with changes in the above 3 parameters.

The sensitivity of HNRT to ETNA parameters has also been performed. Every conceptual reservoir has only 2 parameters that decide the transit time: recession (a) and immobile volume (V). Starting with $a = 0.05$ and $V = 5000\text{mm}$, the values of these 2 parameters have been altered to check their impact on the response of a unit pulse of nitrate sent on 1st August 1968. The above 2 analyses were then compared to check the equivalences/dissimilarities in the two transit time estimation procedures.

3. Results and Discussions:

3.1. Parameter Optimization and implications of storages:

3.1.1. Parameter values: After performing the hydrological analysis mentioned in section 2.2, we found that there is not any equifinality in the physical parameters that rationally and accurately reproduce the fast and slow conceptual stores. Optimal parameters for the best realization are shown in Table 1.

Table 1: Set of optimal physical parameters, namely hydraulic gradient (i), Dirichlet Boundary Conditions of fixed hydraulic heads in the upper and lower boundaries (DBC), hydraulic conductivity (K), total porosity (η), drainable/fillable porosity (η_f), longitudinal hydrodynamic dispersivity (D), length (L) and width (W), that are reproducing concentration breakthroughs equivalent to the calibrated ETNA stores.

Store	i(%)	Dirichlet BC in upper and lower boundaries aka boundary heads	K (m/d)	η	η_f	D (m)	L (m)
Fast	5	Up = 40m Down= 20m	0.202	0.092	0.022	10	385
Slow	5	Up = 40m Down= 20m	0.202	0.565	0.065	10	385

3.1.2. Analysis of parameter significance:

3.1.2.1. Hydrological equivalence:

The hydraulic gradient of 5% is a constant approximation – it changes along the Dupuit-Forchheimer parabola, getting gradually steeper from upper towards lower boundary (at steady state, when no mound is formed). Length of both stores, as mentioned in section 2.2.1, is kept to be equal to the length of the chief diagonal, which can be visualized as a stream-tube carrying all the groundwater. Also, both stores having same length and same boundary heads support the parallel hillslope concept.

The K , η_f and the boundary heads mentioned in Table 1 gave us the mean recession values of 0.024 for fast store and 0.0078 for slow store. We show a sample of the analysis technique for the year 2009 in Figure 3 (b). We also show the reproduced groundwater heads at all 16 points of either optimized store for a period of 2000-2010 in Figure 3 (c). The calibrated mean ETNA recession of fast store was $a_{\text{fast}}=0.0252\pm11.22\%$ and slow store was $a_{\text{slow}}=0.0079\pm13.42\%$ in Fovet et al., 2015. As can be seen, mean recessions for the slow store and the fast store for our optimized box aquifers fall within the bounds obtained by Fovet et al., 2015. This part, as mentioned in the introduction, can be explained by the linkage of Darcy flow to linear reservoir theory (Savenije, 2018). If we want to mathematically represent recession in terms of conventional groundwater parameters, it will be:

$$a = \frac{K}{L\eta_f} \quad \text{Eq(4)}$$

Which comes out to be 0.0238 for fast store and 0.008 for slow store, agreeing with both the calibrated conceptual stores of ETNA and FEFLOW box aquifers. This substantiates the opinion of Savenije, 2018 on equivalence of Darcy equation to linear reservoir equation.

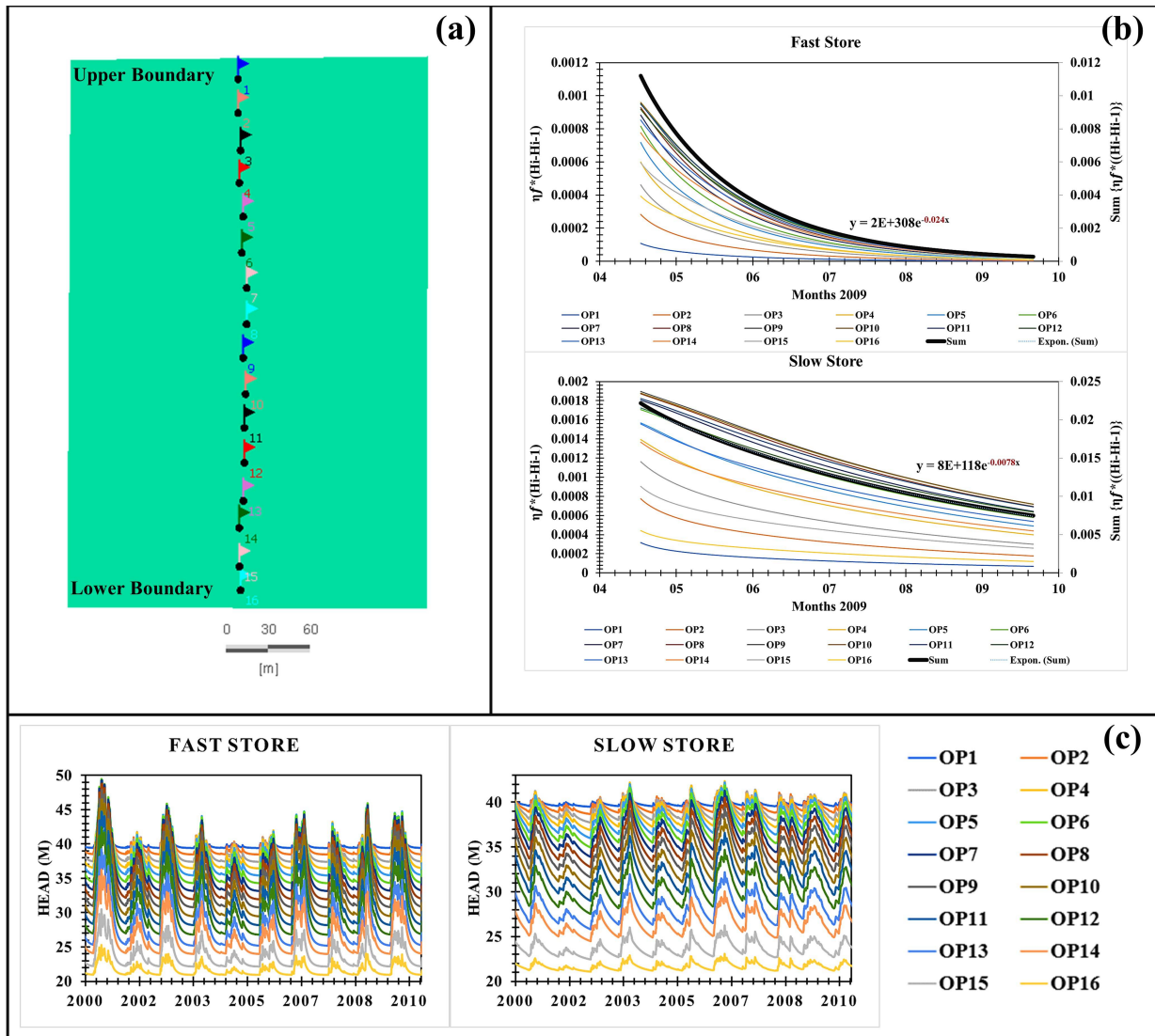


Figure 3: (a) The box catchment with the location of 16 observation points. (b) Illustration of sample recession calculation technique for fast and slow FEFLOW stores for 2009 (April to September). (c) Hydraulic heads at all 16 observation points of both stores for the period 2000-2010.

3.1.2.2. Equivalence in solute transport:

Here apparently K , η_f play the role of seasonality reproduction, and boundary heads and immobile porosity ($\eta - \eta_f$) play the role of dilution. The 3D view of 2D Dupuit-Forchheimer aquifer with

hydraulic head isolines are shown in Figure 4.

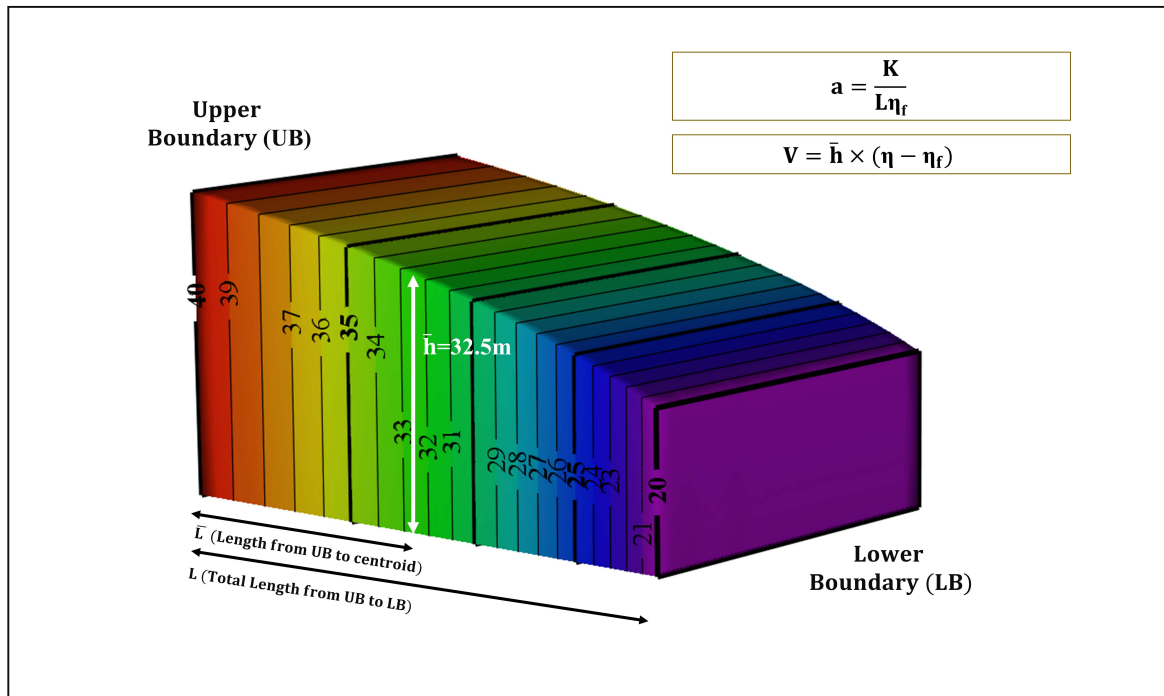


Figure 4: 3D view of optimized 2D synthetic Dupuit-Forchheimer box aquifer showing hydraulic head (m) isoline distribution under steady state, and featuring the dimensional parameters required for a and V calculation.

The geometric centroid of a semi-parabola is at $3/8^{\text{th}}$ distance from the semi-minor axis. In the case of a Dupuit-Forchheimer parabola, one has to count $3/8^{\text{th}}$ of the total number of isolines from the upper boundary, and the head at that corresponding location will be the central head which is demarcated as \bar{h} in Figure 4. For both stores, as shown in Figure 4, a 5% slope is reproduced by a hydraulic head varying from 40m (up) to 20m (down). There are 20 isolines between 40m and 20m DBC heads, so at 7.5 isolines away from 40m DBC we have the isolar centroid where $\bar{h}=32.5\text{m}$. For the fast store, since the immobile porosity ($\eta - \eta_f$) is 0.07, 2.275m is the immobile volume available for mixing which falls within the range of 2354mm \pm 11.01% (Fovet et al., 2015). For the slow store, since the immobile porosity ($\eta - \eta_f$) is 0.5, 16.25m is the immobile volume available for mixing which falls within the range of 16032mm \pm 7.22% (Fovet et al., 2015). So, we have an overall low porosity fast store and high porosity slow store.

So apparently, it looks so that the static storage at the isolar centroids is representative of the immobile or passive mixing volume used in lumped models.

$$V = \bar{h}(\eta - \eta_f) \quad \text{Eq(5)}$$

Figure 5 shows that the output concentration breakthroughs of FEFLOW box aquifers are in well agreement with the originally calibrated conceptual storages. The concentration isoline distributions of the FEFLOW stores across different years during the period of simulation are also shown in Figure 5.

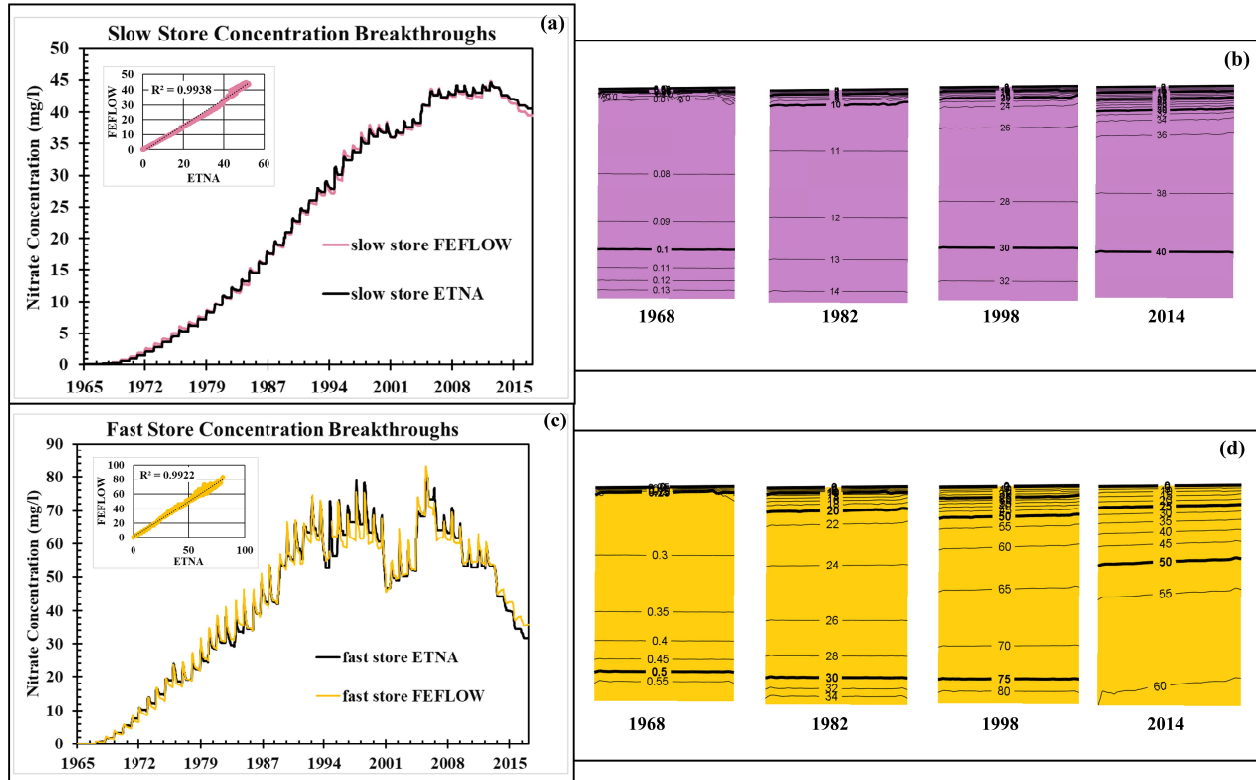


Figure 5: Simulated concentration breakthroughs of slow store (a) and fast store (c) vs corresponding ETNA concentration breakthroughs; concentration isolines in mg/l of slow store (b) and fast store (d) for different intermediate years of the simulation period.

The values of hydrodynamic parameters lie within the broader ranges prescribed from field studies (Martin et al, 2006). However, as mentioned before, our purpose is not to check which configuration of hydrodynamic parameters best represents the catchment behavior. It's rather to check what parameters reproduce the same outputs as a calibrated lumped model so that we can establish a mathematical equivalence.

3.2. Transit time, Age and insights from their sensitivity:

Table 2 shows the HNRT calculated using ETNA, the MTT using FEFLOW, and mean age for fast and slow stores.

Mean age has been calculated as the same way as mean head – the age at age-isolinear centroid (i.e., the age at the location of 3/8th of total number of age isolines from the upper boundary) is the mean age. MTT for slow store is slightly on the higher side because the distribution is long tailed.

Table 2: Transit times calculated using different methods:

Stores	HNRT (ETNA)	MTT (FEFLOW)	Mean age (from Figure 6 charts)
Fast Store	3.22 years	3.15 years	3.08 years
Slow Store	18.44 years	19.3 years	19.17 years

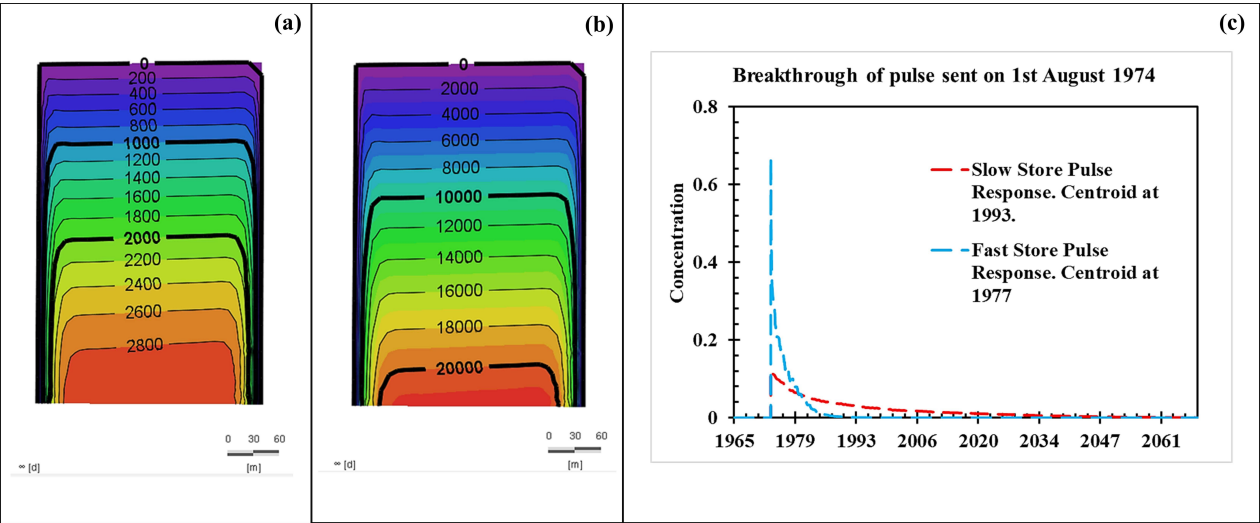


Figure 6: Diagrams showing age distribution in the form of age isolines in days of (a) slow store (b) fast store. (c) Shows responses of unit mass pulses sent on 1st August 1974 (targeting average climatic sequence) for both stores.

Figure 6 shows the age distribution and MTT profiles for different stores (in days). The results of the age sensitivity analysis performed are illustrated in Figure 7. It is seen that with the increase in hydraulic thickness, concentration breakthroughs become more dilute, but the age remains nearly

constant; with the increase in dispersivity, concentration breakthroughs become more dilute, and the mean age reduces; with the increase in immobile porosity, concentration breakthroughs become more dilute, and the mean age increases.

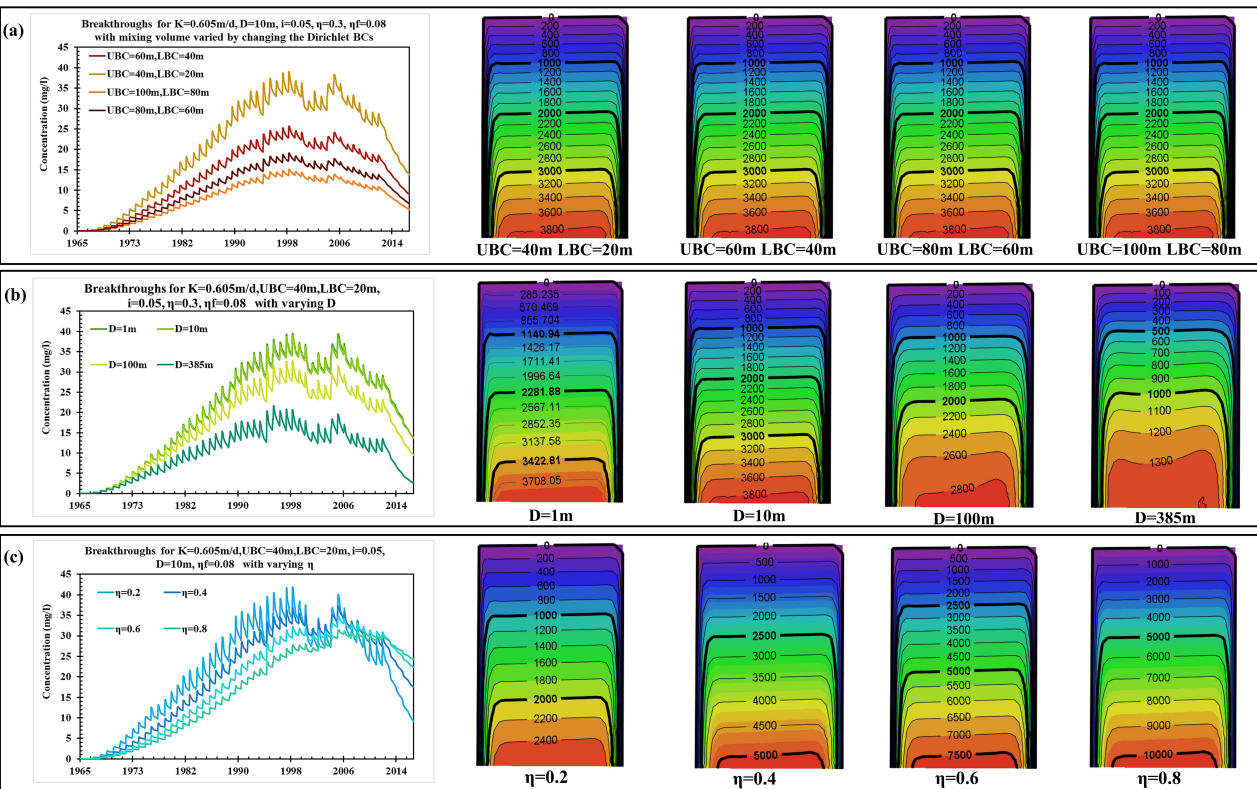


Figure 7: Sensitivity analysis showing changes in concentration breakthroughs in mg/l and age isolines in days with changes in (a) Dirichlet BCs of hydraulic heads, (b) hydrodynamic dispersivity and (c) total porosity keeping the hydraulic gradient, hydraulic conductivity and effective porosity constant.

The results of the HNRT sensitivity analysis performed are illustrated in Figure 8. It is seen that the time taken for the response concentration to reach 50% of steady state concentration is not sensitive to a , but very sensitive to V . Also increase in V reduces the breakthrough concentration – which means transit time in ETNA is proportional to the dilution.

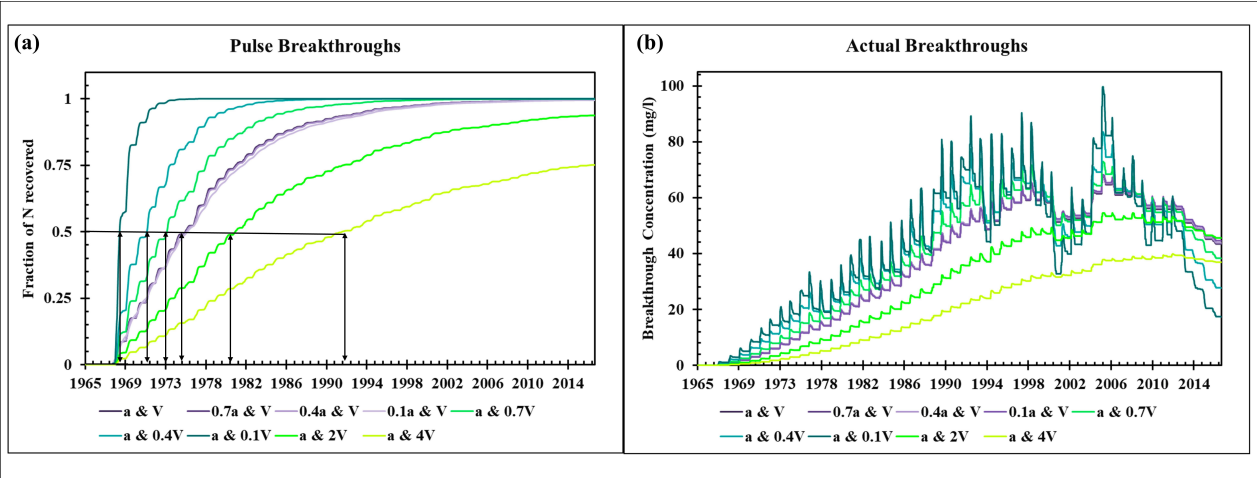


Figure 8: Graphs showing (a) Sensitivity of HNRT (i.e., time taken to recover 50% concentration of a pulse sent on 1st August 1968) and (b) sensitivity of breakthrough concentration with Burns recharge and leachate as loading - with changes in recession and immobile volume (a and V) of one conceptual ETNA box.

The above sensitivity analyses clearly demonstrate that:

- i) The difference of total and drainable porosity ($\eta - \eta_d$) is primarily playing the role of immobile volume in lumped models.
- ii) Lumped models with parallel stores like ETNA do not simulate dispersivity. The phase lag between the responses of the stores arising from different levels of attenuations, when aggregated in their respective proportions, apparently displays a pseudo-dispersion in the concentration breakthrough as illustrated in Figure 9. The reason it is called a pseudo-dispersion is because there is a disparity between the physics of this process and real dispersion - increase in actual dispersion makes the breakthrough profiles more smeared whilst reducing the groundwater age (Figure 7), whereas more pseudo-dispersion increases nitrate transit time because it is associated with higher volume of dead storage available for mixing.

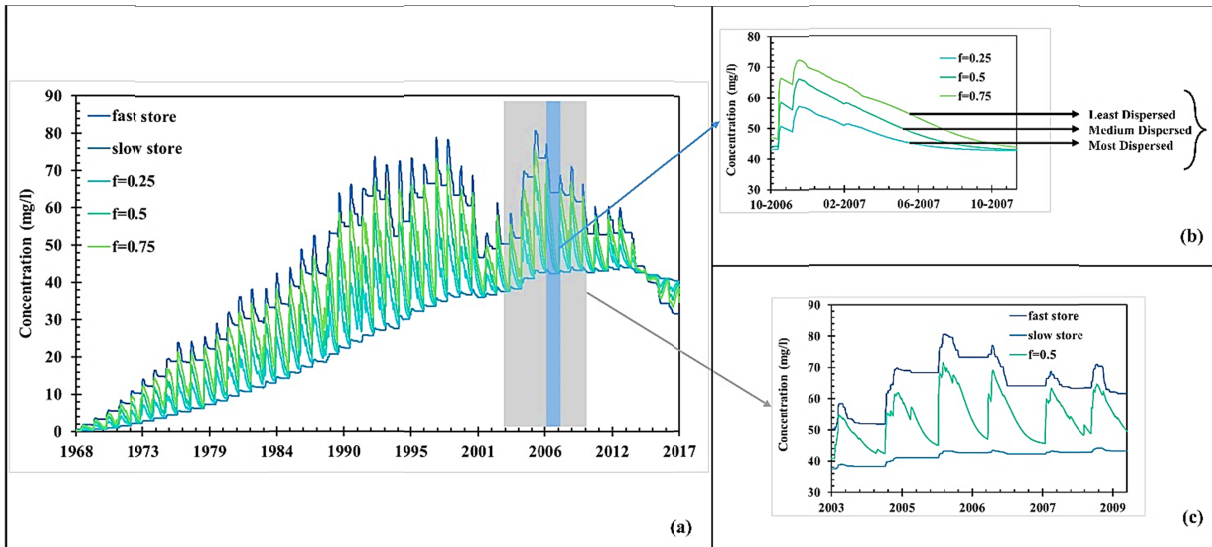


Figure 9: The purpose of the calibrated fraction (f) is illustrated here. (a) Shows the fast and slow store breakthroughs, and the net breakthroughs. (b) Highlights a portion of (a) showing lower f means more dispersion (more smeared and longer tail) and vice versa. (c) Highlights a portion of (a) showing how a phase lag between fast and slow store response in generating the pseudo-dispersion (which explains why lower f means more dispersion as the breakthrough is leaning towards the more lagged slower store).

In Table 3, we provide a mathematical equivalence of the 2 primary lumped store parameters - recession (a , in day^{-1}) and immobile volume (V , in mm). The respective fractions (f) at which they mix is a tricky parameter. For simplicity, in a 2-store lumped model, the parameter f :

- i) Creates a hydrological balance between the faster store which dominates storage accretion and slower store which dominates recession.
- ii) Creates a pseudo-dispersion by combining the concentration breakthrough of less attenuated faster store and more attenuated slower store. This combination, in their respective optimized weights, enabling the lumped model to produce a concentration breakthrough that mimics the real breakthrough which is produced by some degree of dispersivity in the system.

So, f is a purely conceptual calibration parameter, and it is not possible to mathematically connect f to any measurable conventional parameters. In fact, it is not even essential to use 2 stores to model long term groundwater flow and transport (Hrachowitz et al., 2016) – in most HRU based semi-distributed models, groundwater is considered as one calibration chamber (linear reservoir + dead storage) only. Rather, the solute dispersion that is being caused by a dual porosity system is being reproduced by f . Globally, in a lot of catchments we can see that a “thin veneer” of faster flowing water is disproportionately feeding the stream (Berghuijs and Kirchner, 2017) creating a bias towards

shorter transit times of solutes. In ETNA, f (=86.5%) being the contribution of the fast store to the stream nitrate breakthrough, is apparently creating this kind of a bias. The fact that a and V can be expressed in terms of conventional groundwater flow and transport parameters for both stores (fast and slow) with differences just in porosity (total and drainable) is a great insight in the process representation strategy of lumped models.

Table 3: Mathematically connecting lumped store parameters a, V with measurable parameters $K, L, \bar{h}, \eta, \eta_f$

Lumped Store Parameter	The Distributed Equivalent	Source of Evidence
Recession (a)	$\frac{K}{L\eta_f}$ K =Hydraulic conductivity η_f =Fillable porosity L =Length of flow path	Mentioned by Savenije, 2018. Validated in this study. (Section 3.1.2.1, Eq (4))
Immobile Volume (V)	$\bar{h} \times (\eta - \eta_f)$ η =Total porosity \bar{h} = Average hydraulic thickness at 3/8 th isolinear distance (defined as isolinear centroid of Dupuit-Forchheimer parabola) from the upper boundary.	(Section 3.1.2.2, Eq (5)) Figure 4.

So, we have shown that lumped parameters of each individual stores are combinations of actual physical parameters, even if these combinations are not obvious. For a field hydrologist who would like to start forward modelling a pristine catchment using a lumped model, at first, he/she needs to look at the boundary heads and up to what depth flow is significant. This can be inferred from geophysical explorations. Then, even analytically, the Dupuit-Forchheimer aquifer can be constructed and the depth at isolinear centroid can be determined. From such a model it would be easy to determine a and V from Table 3 once the K, η, η_f is determined. Based on the heterogeneity, multiple stores can be considered, and their fractions can be adjusted. For 2 stores, we advise to begin with a value of $f=0.5$ – more pseudo-dispersion will be mimicked by increasing the contribution from the slower store. Apart from knowledge of fundamental hydrodynamic parameters, it is very important to know the length scale of the catchment to avoid equifinality.

4. Conclusion:

The novelty of the study is in the generation of the synthetic experiment – recalibration of the results of a lumped porous media model (calibrated nicely against a real catchment) using a distributed porous media model to establish extrapolatable parametric influence on different variables is a task with a lot of requirements, but the obtained results are supposedly much more authentic than what we might have obtained from dimensional analysis or something similar. The main findings of this study are:

1. The lumped conceptual groundwater flow and transport models have proper physical basis. After detailed analysis it was observed that the fundamental and measurable catchment properties (apart from scale) that affect the hydrologic recession are K and η_f , and the ones that affect mixing (dilution) of solutes are immobile porosity ($\eta - \eta_f$) and mean aquifer thickness. Also, we found that the three proxies of residence time distributions we could estimate from the different modelling approaches - the spatial mean of the age distributions, the mean transit time and the half nitrate recovery time agreed with each other for such lumped (linear reservoir + dead storage) systems.

Furthermore, specific to the calibration exercise that we performed, we found the store with overall lower porosity (mobile and immobile) is the faster store and with overall higher porosity is the slower store - which makes sense because lower porosity means steeper recession and less mixing. It suggests that the idea of dual store conceptual representation of groundwater fundamentally came from the proposition of treating aquifers as dual-porosity systems.

2. Scale is a big issue - all physical representations of lumped parameters are in some way dependent on the catchment dimensions. Lumped conceptual models only operate on dimensions of depth of water column. It is therefore possible for the lumped models to yield the same results for a different set of hydrodynamic parameters for a catchment having different dimensions. Like, for example - transit time of a bigger catchment with low porosity might be same as a smaller catchment with high porosity. It is thus important to a) be extra attentive in deciding the catchment dimensions before using lumped models as forward models and b) to normalize the transit times with catchment dimensions whilst using lumped models for comparative study between catchment response rates.

3. The hydrodynamic dispersion is not accounted for by individual stores of the lumped models. It is quite evident from the age distribution profiles that increase in dispersivity makes the concentration breakthroughs more dilute but at the same time reduces the groundwater age. This is expected based

on the age transport equation. The opposite happens for lumped models where solute transit times are primarily dependent on mixing volumes, and an increase in the mixing volume increases both the dilution and detention time. Dilution is thus a process quite different from hydrodynamic dispersion. The phase lag between the responses of the parallel stores (representing different porosities), when assimilated in their respective proportions (f), apparently displays a synthetic dispersion in the concentration breakthrough due to differences in their respective attenuations. Therefore, a negligible dispersivity of 10m obtained from Gelhar's charts, which shows no difference in breakthrough behavior from zero dispersivity, was maintained across all realizations.

Overall, this study has established that lumped conceptual models used to determine groundwater flow and transport have a genuine physical basis and their empirical parameters have clear mathematical correlation with conventional hydrological parameters. This finding can help in reducing calibration reliance of lumped models, or decreasing calibration uncertainties by giving insights on the parameter ranges, and providing possibilities to scrutinize the effectiveness of obtained parameters. It also indirectly creates a lumped forward modelling potential that can be used to model the flow and transport behavior and solute transit times of catchments that have proper measurements of hydrodynamic properties, but the hydrologic and the breakthrough concentration time series are not long enough to run calibration exercises.

Acknowledgements and Funding:

Funder 1: ANR Ref: ATCHA ANR-16-CE03-0006.

Funder 2: Indian Institute of Science Ref: SP/INRA-17-0002

Code/Data Availability Statement:

All data sets are publicly available in the agrhys repository of INRAE, France.

Link to data: [Grapheur de VIDAÉ \(agrhys.fr\)](https://grapheur.de-vidae.agrhys.fr)

Link to code and user instructions provided in supplementary.

References:

1. Aquilina, Luc, et al. "Nitrate dynamics in agricultural catchments deduced from groundwater dating and long-term nitrate monitoring in surface-and groundwaters." *Science of the total environment* 435 (2012): 167-178.

2. Basu, Nandita B., et al. "Managing nitrogen legacies to accelerate water quality improvement." *Nature Geoscience* 15.2 (2022): 97-105.
3. Basu, Nandita B., et al. "Nutrient loads exported from managed catchments reveal emergent biogeochemical stationarity." *Geophysical Research Letters* 37.23 (2010).
4. Benettin, Paolo, et al. "Transit time estimation in catchments: Recent developments and future directions." *Water Resources Research* 58.11 (2022): e2022WR033096.
5. Berghuijs, Wouter R., and James W. Kirchner. "The relationship between contrasting ages of groundwater and streamflow." *Geophysical Research Letters* 44.17 (2017): 8925-8935.
6. Bhaduri, Baibaswata, et al. "Estimating solute travel times from time series of nitrate concentration in groundwater: Application to a small agricultural catchment in Brittany, France." *Journal of Hydrology* 613 (2022): 128390.
7. Bhaduri, Baibaswata, Sekhar Muddu, and Laurent Ruiz. "An attempt to bridge the gap between physical and conceptual hydrological models used for transit time determination." *EGU General Assembly Conference Abstracts*. 2022.
8. Birkel, Christian, Chris Soulsby, and Doerthe Tetzlaff. "Integrating parsimonious models of hydrological connectivity and soil biogeochemistry to simulate stream DOC dynamics." *Journal of Geophysical Research: Biogeosciences* 119.5 (2014): 1030-1047.
9. Birkel, Christian, Chris Soulsby, and Doerthe Tetzlaff. "Conceptual modelling to assess how the interplay of hydrological connectivity, catchment storage and tracer dynamics controls nonstationary water age estimates." *Hydrological Processes* 29.13 (2015): 2956-2969.
10. Blöschl, Günter, et al. "Twenty-three unsolved problems in hydrology (UPH)—a community perspective." *Hydrological sciences journal* 64.10 (2019): 1141-1158.
11. Burns, I. G. "An equation to predict the leaching of surface-applied nitrate." *The Journal of Agricultural Science* 85.3 (1975): 443-454. Diersch, Hans-Jörg G. *FEFLOW: finite element modeling of flow, mass and heat transport in porous and fractured media*. Springer Science & Business Media, 2013.
12. Duffy, Christopher J. "Dynamical modelling of concentration–age–discharge in watersheds." *Hydrological processes* 24.12 (2010): 1711-1718.
13. Dunn, S. M., et al. "The role of groundwater characteristics in catchment recovery from nitrate pollution." *Hydrology Research* 43.5 (2012): 560-575.

14. Dunn, Sarah M., Jeffrey J. McDonnell, and Kellie B. Vaché. "Factors influencing the residence time of catchment waters: A virtual experiment approach." *Water Resources Research* 43.6 (2007).
15. Ehrhardt, Sophie, et al. "Trajectories of nitrate input and output in three nested catchments along a land use gradient." *Hydrology and Earth System Sciences* 23.9 (2019): 3503-3524.
16. Etcheverry, David, and Pierre Perrochet. "Direct simulation of groundwater transit-time distributions using the reservoir theory." *Hydrogeology Journal* 8.2 (2000): 200-208.
17. Fenicia, Fabrizio, et al. "Assessing the impact of mixing assumptions on the estimation of streamwater mean residence time." *Hydrological Processes* 24.12 (2010): 1730-1741.
18. Fovet, Ophélie, et al. "AgrHyS: An observatory of response times in agro-hydro systems." *Vadose Zone Journal* 17.1 (2018): 1-16.
19. Fovet, Ophélie, et al. "Using long time series of agricultural-derived nitrates for estimating catchment transit times." *Journal of Hydrology* 522 (2015): 603-617.
20. Galloway, James N., et al. "Nitrogen cycles: past, present, and future." *Biogeochemistry* 70 (2004): 153-226.
21. Gelhar, Lynn W., Claire Welty, and Kenneth R. Rehfeldt. "A critical review of data on field-scale dispersion in aquifers." *Water resources research* 28.7 (1992): 1955-1974.
22. Gilmore, Troy E., et al. "Groundwater transit time distribution and mean from streambed sampling in an agricultural coastal plain watershed, North Carolina, USA." *Water Resources Research* 52.3 (2016): 2025-2044.
23. Goode, Daniel J. "Direct simulation of groundwater age." *Water Resources Research* 32.2 (1996): 289-296.
24. Gupta, Hoshin V., Thorsten Wagener, and Yuqiong Liu. "Reconciling theory with observations: elements of a diagnostic approach to model evaluation." *Hydrological Processes: An International Journal* 22.18 (2008): 3802-3813.
25. Howden, Nicholas JK, et al. "Nitrate pollution in intensively farmed regions: What are the prospects for sustaining high-quality groundwater?." *Water Resources Research* 47.6 (2011).
26. Hrachowitz, Markus, et al. "A decade of Predictions in Ungauged Basins (PUB)—a review." *Hydrological sciences journal* 58.6 (2013): 1198-1255.
27. Hrachowitz, Markus, et al. "Transit times—The link between hydrology and water quality at the catchment scale." *Wiley Interdisciplinary Reviews: Water* 3.5 (2016): 629-657.

28. Kirchner, James W. "Getting the right answers for the right reasons: Linking measurements, analyses, and models to advance the science of hydrology." *Water Resources Research* 42.3 (2006).
29. Kirchner, James W., Xiahong Feng, and Colin Neal. "Fractal stream chemistry and its implications for contaminant transport in catchments." *Nature* 403.6769 (2000): 524-527.
30. Kollet, Stefan J., and Reed M. Maxwell. "Integrated surface-groundwater flow modeling: A free-surface overland flow boundary condition in a parallel groundwater flow model." *Advances in Water Resources* 29.7 (2006): 945-958.
31. Li, Li, et al. "Toward catchment hydro-biogeochemical theories." *Wiley Interdisciplinary Reviews: Water* 8.1 (2021): e1495.
32. Małoszewski, Piotr, and Andrzej Zuber. "Determining the turnover time of groundwater systems with the aid of environmental tracers: 1. Models and their applicability." *Journal of hydrology* 57.3-4 (1982): 207-231.
33. Martin, Charlotte, et al. "Modelling the effect of physical and chemical characteristics of shallow aquifers on water and nitrate transport in small agricultural catchments." *Journal of Hydrology* 326.1-4 (2006): 25-42.
34. Martinec, J. "Subsurface flow from snowmelt traced by tritium." *Water Resources Research* 11.3 (1975): 496-498.
35. McDonald, Michael G., and Arlen W. Harbaugh. "The history of MODFLOW." *Ground water* 41.2 (2003): 280.
36. McGuire, Kevin J., and Jeffrey J. McDonnell. "A review and evaluation of catchment transit time modeling." *Journal of Hydrology* 330.3-4 (2006): 543-563.
37. McMillan, Hilary, et al. "Do time-variable tracers aid the evaluation of hydrological model structure? A multimodel approach." *Water Resources Research* 48.5 (2012).
38. Meals, Donald W., Steven A. Dressing, and Thomas E. Davenport. "Lag time in water quality response to best management practices: A review." *Journal of environmental quality* 39.1 (2010): 85-96.
39. Phillips, Fred M., and Maria Clara Castro. "Groundwater dating and residence-time measurements." *Treatise on geochemistry* 5 (2003): 605.
40. Rockström, J., W. Steffen, and K. Noone. "Persson, \AA." *Chapin, FS, Lambin, EF, Lenton, TM, Scheffer, M., Folke, C., Schellnhuber, HJ, others* (2009): 472-475.
41. Ruiz, L., et al. "Effect on nitrate concentration in stream water of agricultural practices in small catchments in Brittany: I. Annual nitrogen budgets." *Hydrology and Earth System Sciences* 6.3 (2002): 497-506.

- 640 42. Savenije, Hubert HG. "HESS Opinions: Linking Darcy's equation to the linear
641 reservoir." *Hydrology and Earth System Sciences* 22.3 (2018): 1911-1916.
- 642 43. Seibert, Jan, and Jeffrey J. McDonnell. "On the dialog between experimentalist and
643 modeler in catchment hydrology: Use of soft data for multicriteria model
644 calibration." *Water Resources Research* 38.11 (2002): 23-1.
- 645 44. Seitzinger, Sybil P., et al. "Global river nutrient export: A scenario analysis of past and
646 future trends." *Global biogeochemical cycles* 24.4 (2010).
- 647 45. Soulsby, Christopher, et al. "Stream water age distributions controlled by storage
648 dynamics and nonlinear hydrologic connectivity: Modeling with high-resolution isotope
649 data." *Water Resources Research* 51.9 (2015): 7759-7776.
- 650 46. Tomer, M. D., and M. R. Burkart. "Long-term effects of nitrogen fertilizer use on ground
651 water nitrate in two small watersheds." *Journal of environmental quality* 32.6 (2003):
652 2158-2171.
- 653 47. Wang, L., et al. "The nitrate time bomb: a numerical way to investigate nitrate storage
654 and lag time in the unsaturated zone." *Environmental Geochemistry and Health* 35
655 (2013): 667-681.
- 656 48. Worrall, F., et al. "The fluvial flux of nitrate from the UK terrestrial biosphere—an
657 estimate of national-scale in-stream nitrate loss using an export coefficient
658 model." *Journal of Hydrology* 414 (2012): 31-39.
- 659 49. Zheng, C., et al. "MT3DMS: Model use, calibration, and validation." *Transactions of the*
660 *ASABE* 55.4 (2012): 1549-1559.
- 661